

Editor
Ya-Qiu Jin

Wave Propagation, Scattering and Emission in Complex Media



Science Press
Beijing, China



World Scientific
Singapore City, Singapore

WAVE PROPAGATION, SCATTERING AND EMISSION IN COMPLEX MEDIA

Editor: Ya-Qiu Jin



Science Press



World Scientific

Responsible Editors: Bin PENG and Lu QIU

Copyright © 2004 by Science Press and World Scientific Publishing Co. Pte. Ltd.
Published by Science Press, and World Scientific

Science Press
16 Donghuangchenggen North Street
Beijing, 100717
P.R. China

World Scientific Publishing Co. Pte. Ltd.
5 Toh Tuck Link
Singapore, 596224

Printed in Beijing.

All rights reserved.

This book, or parts thereof, may not be reproduced in any form or by any means, electronic or mechanical, including photocopying, recording or any information storage and retrieval system now known or to be invented, without written permission from the Publishers.

ISBN 7-03-012464-2 (Beijing)
ISBN 981-238-771-4 (Singapore)

Preface

Electromagnetic wave propagation, scattering and emission are the physics basis for modern information technology. Great advances of satellite-borne remote sensing, wireless communication, and other information high technology during recent decades have promoted extensive studies on electromagnetic fields and waves, such as theoretical modeling, experiments and data validation, numerical simulation and inversion. To exchange most recent research achievements and discuss the future topics, the International Workshop on Wave Propagation, Scattering and Emission (WPSE2003) as an international forum was scheduled to be held in Shanghai, China, 1-4 June 2003.

This workshop was sponsored by the IEEE Geoscience and Remote Sensing Society, the USA Electromagnetic Academy, PIERS, the Fudan University, and the City University of Hong Kong. Our many colleagues, especially many distinguished scientists in the world, enthusiastically prepared their presentations for the WPSE. However, unfortunately, due to the SARS infection in the spring season 2003 in some places of Asia, this workshop had to be cancelled.

To meet the goal of our international forum, we edit this book to enclose some full papers, which cover seven areas:

1. Polarimetric scattering and SAR imagery,
2. Scattering from randomly rough surfaces,
3. Electromagnetics of complex materials,
4. Scattering from complex targets,
5. Radiative transfer and remote sensing,
6. Wave propagation and wireless communication,
7. Computational electromagnetics.

I hope this book as a good reference would benefit to our colleagues to learn and exchange the research progress in this rapidly developing area of information technology.

We are very grateful to that all authors for their excellent contributions and make this book publication possible.

This book is financially supported by Ministry of Science and Technology of China via the China State Key Basic Research Project 2001CB309400, the National Natural Science Foundation of China, and Shanghai Magnolia Foundation.

Ya-Qiu Jin

WPSE2003 Chairman

Center for Wave Scattering and Remote Sensing

Fudan University

Shanghai

Contents

Preface

I. Polarimetric Scattering and SAR Imagery

- EM Wave Propagation and Scattering in Polarimetric SAR Interferometry *S.R. Cloude* (3)
- Terrain Topographic Inversion from Single-Pass Polarimetric SAR Image Data by Using
Polarimetric Stokes Parameters and Morphological Algorithm *Y.Q. Jin, L. Luo* (29)
- Road Detection in Forested Area Using Polarimetric SAR
..... *G.W. Dong, J. Yang, Y.N. Peng, C. Wang, H. Zhang* (38)
- Research on Some Problems about SAR Radiometric Resolution
..... *G. Dong, M.H. Zhu, X.Y. Tian, J.Y. Fan* (45)
- A Fast Image Matching Algorithm for Remote Sensing Applications
..... *Z.Q. Hou, C.Z. Han, L. Zheng, X. Kang* (51)
- A New Algorithm of Noised Remote Sensing Image Fusion Based on Steerable Filters
..... *X. Kang, L. Zheng, C.Z. Han, Q. Ma, C.H. Zhao* (56)
- Adaptive Noise Reduction of InSAR Data Based on Anisotropic Diffusion Models and Their
Applications to Phase Unwrapping *C. Wang, X. Gao, H. Zhang* (63)

II. Scattering from Randomly Rough Surfaces

- Modeling Tools for Backscattering from Rough Surfaces *A.K. Fung, K.S. Chen* (75)
- Pseudo-Nondiffracting Beams from Rough Surface Scattering
..... *E.R. Méndez, T.A. Leskova, A.A. Maradudin* (100)
- Surface Roughness Clutter Effects in GPR Modeling and Detection
..... *C. Rappaport* (119)
- Scattering from Rough Surfaces with Small Slopes *M. Saillard, G. Soriano* (128)
- Polarization and Spectral Characteristics of Radar Signals Reflected by Sea-surface
..... *V.A. Butko, V.A. Khlusov, L.I. Sharygina* (134)
- Simulation of Microwave Scattering from Wind-Driven Ocean Surfaces
..... *M.Y. Xia, C.H. Chan, G. Soriano, M. Saillard* (139)
- HF Surface Wave Radar Tests at the Eastern China Sea
..... *X.B. Wu, F. Cheng, S.C. Wu, Z.J. Yang, B.Y. Wen,
Z.H. Shi, J.S. Tian, H.Y. Ke, H.T. Gao* (151)

III. Electromagnetics of Complex Materials

Wave Propagation in Plane-Parallel Metamaterial and Constitutive Relations	<i>A. Ishimaru, J. Thomas, S.W. Lee, Y. Kuga</i> (163)
Two Dimensional Periodic Approach for the Study of Left-Handed Metamaterials	<i>T.M. Grzegorzczuk, L. Ran, X. Zhang, K. Chen, X. Chen, J.A. Kong</i> (182)
Numerical Analysis of the Effective Constitutive Parameters of a Random Medium Containing Small Chiral Spheres	<i>Y. Nanbu, T. Matsuoka, M. Tateiba</i> (194)
Wave Propagation in Inhomogeneous Media: From the Helmholtz to the Ginzburg -Landau Equation	<i>M. Gitterman</i> (203)
Transformation of the Spectrum of Scattered Radiation in Randomly Inhomogeneous Absorptive Plasma Layer	<i>G.V. Jandieri, G.D. Aburjania, V.G. Jandieri</i> (207)
Numerical Analysis of Microwave Heating on Saponification Reaction	<i>K. Huang, K. Jia</i> (215)
IV. Scattering from Complex Targets	
Analysis of Electromagnetic Scattering from Layered Crossed-Gratings of Circular Cylinders Using Lattice Sums Technique	<i>K. Yasumoto, H. T. Jia</i> (225)
Scattering by a Body in a Random Medium	<i>M. Tateiba, Z.Q. Meng, H. El-Ocla</i> (240)
A Rigorous Analysis of Electromagnetic Scattering from Multilayered Crossed-arrays of Metallic Cylinders	<i>H. T. Jia, K. Yasumoto</i> (250)
Vector Models of Non-stable and Spatially-distributed Radar Objects	<i>A. Surkov, V. A. Khlusov, L. Ligthart, G. Sharygin</i> (263)
Simulation of Algorithm of Orthogonal Signals Forming and Processing Used to Estimate Back Scattering Matrix of Non-stable Radar Objects	<i>D. Nosov, A. Surkov, V. A. Khlusov, L. Ligthart, G. Sharygin</i> (269)
New Features of Scattering from a Dielectric Film on a Reflecting Metal Substrate	<i>Z.H. Gu, I.M. Fuks, M. Ciftan</i> (281)
A Higher Order FDTD Method for EM Wave Propagation in Collision Plasmas	<i>S.B. Liu, J.J. Mo, N.C. Yuan</i> (294)
V. Radiative Transfer and Remote Sensing	
Simulating Microwave Emission from Antarctica Ice Sheet with a Coherent Model	<i>M. Tedesco, P. Pampaloni</i> (303)
Scattering and Emission from Inhomogeneous Vegetation Canopy and Alien Target by Using Three-Dimensional Vector Radiative Transfer (3D-VRT) Equation	<i>Y.Q. Jin, Z. C. Liang</i> (311)
Analysis of Land Types Using High-resolution Satellite Images and Fractal Approach	<i>H.G. Zhang, W.G. Huang, C.B. Zhou, D.L. Li, Q.M. Xiao</i> (324)
Data Fusion of RADARSAT SAR and DMSP SSM/I for Monitoring Sea Ice of China's	

Bohai Sea	<i>Y.Q. Jin</i> (332)
-----------------	-----------------------

Retrieving Atmospheric Temperature Profiles from Simulated Microwave Radiometer Data with Artificial Neural Networks	<i>Z. G. Yao, H. B. Chen</i> (341)
---	------------------------------------

VI. Wave Propagation and Wireless Communication

Wireless Propagation in Urban Environments: Modeling and Experimental Verification	<i>D. Erricolo, P.L.E. Uslenghi, Y. Xu, Q. W. Tan</i> (353)
---	---

An Overview of Physics-based Wave Propagation in Forested Environment	<i>K. Sarabandi, I. Koh</i> (367)
--	-----------------------------------

Angle-of-arrival Fluctuations due to Meteorological Conditions in the Diffraction Zone of C-band Radio Waves, Propagated over the Ground Surface	<i>T.A.Tyufilina, A.A. Mescheryakov, M.V. Krutikov</i> (373)
--	--

Simulating Radio Channel Statistics Using Ray Based Prediction Codes	<i>H.L. Bertoni</i> (380)
--	---------------------------

Measurement and Simulation of Ultra Wideband Antenna Elements	<i>W. Sörgel, W. Wiesbeck</i> (389)
--	-------------------------------------

The Experimental Investigation of a Ground-placed Radio Complex Synchronization System	<i>V.P. Denisov, V.Y. Lebedev, D.E. Kolesnikov, V.G. Kornienko, M.V. Krutikov</i> (397)
---	---

VII. Computational Electromagnetics

Analysis of 3-D Electromagnetic Wave Scattering with the Krylov Subspace FFT Iterative Methods.....	<i>R.S. Chen, Z.H. Fan, D.Z. Ding, E.K.N. Yung</i> (407)
--	--

Sparse Approximate Inverse Preconditioned Iterative Algorithm with Block Toeplitz Matrix for Fast Analysis of Microstrip Circuits	<i>L. Mo, R.S. Chen, E. K.N. Yung</i> (417)
--	---

An Efficient Modified Interpolation Technique for the Translation Operators in MLFMA	<i>J. Hu, Z.P. Nie, G.X. Zou</i> (426)
---	--

Efficient Solution of 3-D Vector Electromagnetic Scattering by CG-MLFMA with Partly Approximate Iteration	<i>J. Hu, Z.P. Nie</i> (433)
--	------------------------------

The Effective Constitution at Interface of Different Media	<i>L.G. Zheng, W.X. Zhang</i> (440)
---	-------------------------------------

Novel Basis Functions for Quadratic Hexahedral Edge Element	<i>P. Liu, J. D. Xu, W. Wan, Y.Q. Jin</i> (445)
--	---

A Higher Order FDTD Method for EM Wave Propagation in Collision Plasmas	<i>S.B. Liu, J.J. Mo, N.C. Yuan</i> (454)
--	---

Attenuation of Electric Field Eradiated by Underground Source	<i>J. P. Dong, Y. G. Gao</i> (460)
--	------------------------------------

Author Index	(465)
---------------------------	-------

I. Polarimetric Scattering and SAR Imagery

EM Wave Propagation and Scattering in Polarimetric SAR Interferometry

Shane R Cloude,
AEL Consultants,
Granary Business Centre, Cupar, KY15 5YQ, Scotland, UK
Tel/Fax : (44) 1334 652919/654192, Email: scloude@aelc.demon.co.uk

Abstract In this paper we develop a multi-layer coherent polarimetric vegetation scattering model to investigate physical parameter estimation using fully polarimetric multi-baseline multi-frequency radar interferometry. It is shown that 2-layer model inversion for single baseline/single frequency sensors requires regularisation to remove multiple solutions. Traditionally this is achieved by using assumptions about polarimetric ground scattering ratios. By employing dual frequency or multi-baseline data these multiple solutions can be removed. However, the model inversion becomes ill-conditioned unless the correct baseline and frequency ratios are employed. In this paper we show how wave propagation and scattering models can be used to help devise robust inversion methods for land surface parameter estimation.

1. Introduction

In previous studies we have shown that by using single baseline polarimetric interferometry (SBPI), estimates of vegetation height and ground topography can be obtained without the need for external reference DEMs or data specific regression formulae [1,2,3,4]. However, the robustness of this inversion process is based on the assumption that in at least one (not all) of the observed polarisation channels, the ratio of ground to volume scattering is small (typically less than -10dB for 10% height accuracy). We have found two main limitations to this SBPI approach. The first is that the polarisation response of the sub-canopy ground cannot be properly estimated, as by definition the ground scattering is assumed zero in one of the channels. Hence, if we could devise a sensor capable of estimating the full polarisation response of the underlying surface then this would lead to the following improvements:

- a) free the technique from the need to assume a directly observable volume coherence
- b) enable several interesting extensions of the method such as to sub-canopy moisture and surface roughness estimation.

A second limitation of SBPI is the inability of single baseline techniques to determine vertical structure. The model assumes a vertically uniform spatial density of scatterers which maps into an exponentially weighted integral to determine the coherence. However, many trees show important variations in canopy density and if we could devise a sensor configuration capable of estimating this structure, then we could augment the height information for improved species and biomass related studies. In either case we need to increase the number of observations in the data. There are several possible ways to do this. Dual frequency or multiple angles of incidence are important examples. The use of dual baseline regularisation has already been treated in [5] and the use of an extra frequency channel in [6]. Here we review the background to this important topic and highlight the key

contribution made by electromagnetic wave propagation and scattering models to the development of quantitative parameter estimation algorithms.

2. COHERENT VECTOR INSAR MODEL

The key observable of interest in interferometry is phase. The phase difference between signals from positions 1 and 2 and is non-zero due to the slightly different propagation path lengths Δr . This phase has the form shown in equation 1 (where B_n is the normal component of the baseline)

$$\exp(i2k\Delta r) \approx \exp\left(\frac{4\pi}{\lambda} \delta\theta m\right) \approx \exp\left(\frac{4\pi B_n}{\lambda R} m\right) \quad (1)$$

where $\theta \approx B_n/R$ if $R \gg B$ and the co-ordinate m is defined as normal to the slant range direction. Transforming to the surface y, z co-ordinates using the mean angle of incidence θ we can also express equation 1 in the modified form $\exp(i\phi(y, z))$ where

$$\phi(y, z) = y\left(\frac{2kB_n \cos \theta}{R} - 2\Delta k \sin \theta\right) + z\left(\frac{2kB_n \sin \theta}{R} + 2\Delta k \cos \theta\right) \quad \Delta k = \frac{kB_n}{R \tan \theta} \quad (2)$$

In equation 2 we have further included the possibility of making a wavenumber shift Δk between the two images. This shift can best be derived using a k -space representation of interferometry as shown in figure 1 [12, 13]. Here the radial co-ordinate is the wavenumber $k = \pi/\lambda$ and the polar co-ordinate the angle of incidence. By making a frequency shift Δf to one of the signals then we see that we can equalise the k_y components of the wavenumber.

As is apparent from equation 2, we can then always remove the 'y' dependence of the phase ϕ by choosing Δk based on the geometry of the system. In this case the interferometric phase depends only on the height of the scatterers above the reference plane (the z co-ordinate) i.e. we need consider only the volume scattering contributions.

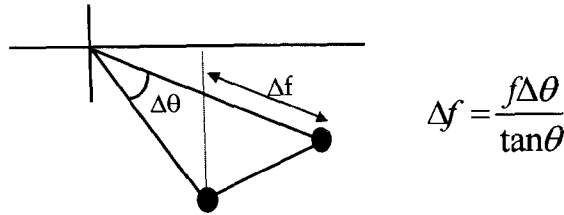


Figure 1 : K-space representation of radar interferometry

To study decorrelation in the 'z' direction, we then define an effective vertical propagation constant using 1 and 2 so that

To study decorrelation in the 'z' direction, we then define an effective vertical propagation constant using 1 and 2 so that

$$k_z = \frac{4\pi\delta\theta}{\lambda \sin \theta} \approx \frac{4\pi B_n}{\lambda R \sin \theta} \quad (3)$$

A scatterer that changes in height by Δz will then have an associated phase change of $k_z \Delta z$. In foliage examples there will be a random distribution of scatterers in the vertical direction. This will cause fluctuations in the phase which are manifest as a drop in the interferometric coherence γ [7,8]. In polarimetric systems we have 3 channels of complex data at positions 1 and 2 (HH, VV and HV). Hence to generate the appropriate coherence we need first to project the 3 channels onto a unitary weight vector \underline{w}_1 to generate a complex scalar s_1 as shown in equation 4. Similarly we can define a different weight vector \underline{w}_2 and scalar s_2 at position 2. The interferometric coherence is then defined from the normalised product of the scalar projections as shown in equation 4

$$\begin{aligned} & \left. \begin{aligned} s_1 &= \underline{w}_1^{*T} \underline{k}_1 \\ s_2 &= \underline{w}_2^{*T} \underline{k}_2 \end{aligned} \right\} \\ \Rightarrow & \left\{ \begin{aligned} \gamma &= \frac{|\langle s_1 s_2^* \rangle|}{\sqrt{\langle s_1 s_1^* \rangle \langle s_2 s_2^* \rangle}} = \frac{|\underline{w}_1^{*T} \underline{\Omega}_{12} \underline{w}_2|}{\sqrt{\underline{w}_1^{*T} T_{11} \underline{w}_1 \underline{w}_2^{*T} T_{22} \underline{w}_2}} \quad 0 \leq \gamma \leq 1 \\ \phi &= \arg(s_1 s_2^*) = \arg(\underline{w}_1^{*T} \underline{\Omega}_{12} \underline{w}_2) \end{aligned} \right. \quad (4) \end{aligned}$$

We see that the coherence and phase can be expressed in terms of a vector of scattering coefficients \underline{k} and 3x3 block elements of a 6 x 6 coherency matrix $[P]$ as defined in equation 5

$$[P] = \left\langle \begin{bmatrix} \underline{k}_1 \\ \underline{k}_2 \end{bmatrix} \begin{bmatrix} \underline{k}_1^{*T} & \underline{k}_2^{*T} \end{bmatrix} \right\rangle = \begin{bmatrix} [T_{11}] & [\Omega_{12}] \\ [\Omega_{12}]^{*T} & [T_{22}] \end{bmatrix} \quad (5)$$

In the presence of speckle [11,24], the 6 dimensional coherent polarimetric signal can then be modelled as a multi-variate Gaussian distribution of the form shown in equation 6

$$\underline{u} = \begin{bmatrix} \underline{k}_1 \\ \underline{k}_2 \end{bmatrix} \Rightarrow p(\underline{u}) = \frac{1}{\pi^6 \det([P])} e^{-\underline{u}^T [P]^{-1} \underline{u}} \quad (6)$$

Here again the matrix $[P]$ determines the fluctuation statistics of the signals. Hence to evaluate the coherence [14] for arbitrary polarisation, we need to estimate the block matrices $[T]$ and $[\Omega]$. It is here that use can be made of EM wave propagation and scattering models.

For example, in many vegetation problems the scatterers in a volume have some residual

orientation correlation due to their natural structure (branches in a tree canopy) or due to agriculture (oriented corn stalks). In this case the volume has two eigen-propagation states *a* and *b* (which we assume are unknown but orthogonal linear polarisations). Only along these eigenpolarisations is the propagation simple, in the sense that the polarisation state does not change with depth into the volume. If there is some mismatch between the radar co-ordinates and the medium's eigenstates then a very complicated situation arises where the polarisation of the incident field changes as a function of distance into the volume [9,10]. By assuming that the medium has reflection symmetry about the (unknown) axis of its eigenpolarisations, we obtain a polarimetric coherency matrix $[T]$ and corresponding covariance matrix $[C]$ for backscatter from the volume as shown in equation 7 [2,9]

$$[T] = \begin{bmatrix} t_{11} & t_{12} & 0 \\ t_{12}^* & t_{22} & 0 \\ 0 & 0 & t_{33} \end{bmatrix} \Leftrightarrow [C] = \begin{bmatrix} c_{11} & 0 & c_{13} \\ 0 & c_{22} & 0 \\ c_{13}^* & 0 & c_{33} \end{bmatrix} \quad (7)$$

We can now obtain an expression for the matrices $[T_{11}]$ and $[\Omega_{12}]$ for an oriented volume extending from $z = z_0$ to $z = z_0 + h_v$ as vector volume integrals as shown in equation 8

$$\begin{aligned} [\Omega_{12}] &= e^{-\frac{(\sigma_a + \sigma_b)h_v}{\cos\theta_o}} e^{i\phi(z_o)} R(2\beta) \left\{ \int_0^{h_v} e^{ik_z z'} e^{\frac{(\sigma_a + \sigma_b)z'}{\cos\theta_o}} P(\tau) T P(\tau^*) dz \right\} R(-2\beta) \\ [T_{11}] &= e^{-\frac{(\sigma_a + \sigma_b)h_v}{\cos\theta_o}} R(2\beta) \left\{ \int_0^{h_v} e^{\frac{(\sigma_a + \sigma_b)z'}{\cos\theta_o}} P(\tau) T P(\tau^*) dz \right\} R(-2\beta) \end{aligned} \quad (8)$$

where for clarity we have dropped the brackets around matrices inside the integrals and defined R as a rotation matrix to allow for mismatch between the radar co-ordinates and the projection of the eigenstates into the polarisation plane (equation 9).

$$R(\beta) = \begin{bmatrix} 1 & 0 & 0 \\ 0 & \cos\beta & \sin\beta \\ 0 & -\sin\beta & \cos\beta \end{bmatrix} \quad (9)$$

Differential propagation through the medium is modelled as a matrix transformation as shown in equation 10, with the complex differential propagation constant shown in equation 11

$$P(\tau) T P(\tau^*) = \begin{bmatrix} \cosh\tau & \sinh\tau & 0 \\ \sinh\tau & \cosh\tau & 0 \\ 0 & 0 & 1 \end{bmatrix} \begin{bmatrix} t_{11} & t_{12} & 0 \\ t_{12}^* & t_{22} & 0 \\ 0 & 0 & t_{33} \end{bmatrix} \begin{bmatrix} \cosh\tau^* & \sinh\tau^* & 0 \\ \sinh\tau^* & \cosh\tau^* & 0 \\ 0 & 0 & 1 \end{bmatrix} \quad (10)$$

$$\tau = \nu z = \left(\frac{\sigma_a - \sigma_b}{2} + ik(\chi_a - \chi_b) \right) \frac{z'}{\cos\theta_o} \quad (11)$$

This now enables us to generate the coherence for any choice of weight vector \underline{w} , in equation 4. However we are often more interested in the maximum variability of coherence with changes in \underline{w} and so we employ the coherence maximiser, which requires solution of an eigenvalue problem as shown in equation 12 [1,3]

$$\left. \begin{aligned} [T_{22}^{-1}] [\Omega_{12}]^* [T_{11}^{-1}] [\Omega_{12}] \underline{w}_2 &= \lambda \underline{w}_2 \\ [T_{11}^{-1}] [\Omega_{12}] [T_{22}^{-1}] [\Omega_{12}]^* \underline{w}_1 &= \lambda \underline{w}_1 \end{aligned} \right\} 0 \leq \lambda = \gamma_{opt}^2 \leq 1 \quad (12)$$

The eigenvalues of this matrix then indicate the maximum change of coherence with polarisation. As the eigenvalues are invariant to unitary transformations of the vector \underline{k} we can replace $[T]$ by $[C]$ in equation 12. To account for the effects of propagation on the polarimetric response of an oriented volume, it is simpler to employ the covariance $[C]$ rather than the coherency matrix $[T]$. For a general oriented volume we then have from 6,7 and 8

$$\begin{aligned} C_{11} &= \begin{bmatrix} c_{11}I_1 & 0 & c_{13}I_2 \\ 0 & c_{22}I_3 & 0 \\ c_{13}^*I_2^* & 0 & c_{33}I_4 \end{bmatrix} \\ \Rightarrow C_{11}^{-1} &= \frac{1}{f} \begin{bmatrix} c_{33}I_4 & 0 & -c_{13}I_2 \\ 0 & \frac{f}{c_{22}I_3} & 0 \\ -c_{13}^*I_2^* & 0 & c_{11}I_1 \end{bmatrix} \end{aligned} \quad (13)$$

where $f = (c_{11}c_{33} - c_{13}c_{13}^*)I_1I_4$ and similarly for the Ω matrix we can write

$$\Omega_{12} = e^{i\phi(z_v)} \begin{bmatrix} c_{11}I_5 & 0 & c_{13}I_6 \\ 0 & c_{22}I_7 & 0 \\ c_{13}^*I_8 & 0 & c_{33}I_9 \end{bmatrix} \quad (14)$$

Note that Ω_{12} is neither symmetric nor Hermitian. The integrals $I_1 - I_9$ are defined as [5]

$$\begin{aligned} I_1 &= \int_0^{h_v} e^{2\sigma_a z} dz & I_2 &= \int_0^{h_v} e^{2(k_a + k_b^*)z} dz & I_3 &= \int_0^{h_v} e^{(\sigma_a + \sigma_b)z} dz & I_4 &= \int_0^{h_v} e^{2\sigma_b z} dz & I_5 &= \int_0^{h_v} e^{ik_z} e^{2\sigma_a z} dz \\ I_6 &= \int_0^{h_v} e^{ik_z} e^{2(k_a + k_b^*)z} dz & I_7 &= \int_0^{h_v} e^{ik_z} e^{(\sigma_a + \sigma_b)z} dz & I_8 &= \int_0^{h_v} e^{ik_z} e^{2(k_b + k_a^*)z} dz & I_9 &= \int_0^{h_v} e^{ik_z} e^{2\sigma_b z} dz \end{aligned} \quad (15)$$

and k_z is defined in equation 3, k_a , k_b are the complex propagation constants of the eigenpolarisation states and σ are the real extinction rates in the medium. Hence the first part of the optimisation matrix (equation 12) has the form

$$C_{11}^{-1}\Omega_{12} = \frac{e^{i\phi(z_o)}}{f} \begin{bmatrix} c_{33}I_4 & 0 & -c_{13}I_2 \\ 0 & \frac{f}{c_{22}I_3} & 0 \\ -c_{13}^*I_2^* & 0 & c_{11}I_1 \end{bmatrix} \begin{bmatrix} c_{11}I_5 & 0 & c_{13}I_6 \\ 0 & c_{22}I_7 & 0 \\ c_{13}^*I_8 & 0 & c_{33}I_9 \end{bmatrix} \quad (16)$$

which is diagonal if $I_4I_6 - I_2I_9 = I_8I_1 - I_2^*I_5 = 0$. From equation 15 we can easily show that both equations are satisfied for arbitrary medium parameters as we have

$$I_4I_6 = \int_0^{h_v} e^{2\sigma_b z} e^{ik_z} e^{2(k_a + k_b^*)z} dz = I_2I_9$$

$$I_8I_1 = \int_0^{h_v} e^{2\sigma_a z} e^{ik_z} e^{2(k_b + k_a^*)z} dz = I_2^*I_5 \quad (17)$$

$$\tilde{\gamma}_1 = f(\sigma_a) = \frac{2\sigma_a e^{i\phi(z_o)}}{\cos\theta_o(e^{2\sigma_a h_v / \cos\theta_o} - 1)} \int_0^{h_v} e^{ik_z z} e^{\frac{2\sigma_a z}{\cos\theta_o}} dz'$$

$$\tilde{\gamma}_2 = f(\sigma_a, \sigma_b) = \frac{(\sigma_a + \sigma_b) e^{i\phi(z_o)}}{\cos\theta_o(e^{(\sigma_a + \sigma_b) h_v / \cos\theta_o} - 1)} \int_0^{h_v} e^{ik_z z} e^{\frac{(\sigma_a + \sigma_b)z}{\cos\theta_o}} dz'$$

$$\tilde{\gamma}_3 = f(\sigma_b) = \frac{2\sigma_b e^{i\phi(z_o)}}{\cos\theta_o(e^{2\sigma_b h_v / \cos\theta_o} - 1)} \int_0^{h_v} e^{ik_z z} e^{\frac{2\sigma_b z}{\cos\theta_o}} dz' \quad (18)$$

The optimum coherence values can then be calculated as shown in equation 18. It follows from the above that $K_c = C_{11}^{-1}\Omega_{12}C_{11}^{-1}\Omega_{12}^*$ is also diagonal and hence by using the relationship between [T] and [C] we can show that the eigenvectors of $K = T_{11}^{-1}\Omega_{12}T_{11}^{-1}\Omega_{12}^*$ are functions of β as

$$w_1 = \frac{1}{\sqrt{2}} \begin{bmatrix} 1 \\ -\cos 2\beta \\ \sin 2\beta \end{bmatrix} \quad w_2 = \begin{bmatrix} 0 \\ \sin 2\beta \\ \cos 2\beta \end{bmatrix} \quad w_3 = \frac{1}{\sqrt{2}} \begin{bmatrix} 1 \\ \cos 2\beta \\ -\sin 2\beta \end{bmatrix} \quad (19)$$

Equation 18 shows that the maximum coherence is obtained for the medium eigenpolarisation with the highest extinction. The lowest coherence is then obtained for the orthogonal polarisation that has lower extinction and hence better penetration into the vegetation. The cross polar channel which propagates into the volume on one eigenpolarisation and out on the other has a coherence between these two extremes.

However, in real applications forest cover will often be random and any orientation effects are likely to be weak. For this reason we must consider a special case of equation 18 when the vegetation shows full azimuth symmetry in the plane of polarisation. In this case there can, by definition, be no preferred β angle in equation 19 and hence the coherency matrix for the volume must be diagonal with 2 degenerate eigenvalues of the form [3]

$$[T_v] = m_v \begin{bmatrix} 1 & 0 & 0 \\ 0 & \eta & 0 \\ 0 & 0 & \eta \end{bmatrix} \quad 0 \leq \eta \leq 1 \quad (20)$$

where η depends on the particle shape in the volume and on the presence of multiple scattering. If there is no distinction between the eigenvectors in equation 19 then the eigenvalues in equation 18 must become equal. This arises when $\sigma_a = \sigma_b = \sigma$ i.e. when the extinction in the medium becomes independent of polarisation. In this case volume scattering alone leads to equal eigenvalues in 12 and hence the coherence is no longer a function of polarisation. The situation in practice is made more complicated because some penetration of the vegetation occurs and combined surface and volume scattering occurs. It is well known that surface scattering is strongly polarisation dependent and hence in practice we need to extend the above argument to a multi-layer model.

3. MULTI-LAYER COHERENT SCATTERING MODEL

We consider a general multi-layer oriented random media problem as shown schematically in figure 2. We assume that each layer is composed of a cloud of identical spheroidal particles, where the density of each layer is tenuous enough so that we can ignore reflections at the boundaries between layers. We further assume that we can ignore any refraction at the boundaries between the layers, as justified in [4]. We assume that the propagation eigenstates are orthogonal linear polarisations, but allow for the fact that they may not be aligned with the radar h and v axes.

In order to assess the complexity of the inverse problem consider the following argument. According to our model, each layer is characterised by a set of 9 parameters,

- β - orientation of the eigen-propagation states with respect to the radar co-ordinate system
- h_v - Layer Thickness in metres
- ϕ_{z_0} - Interferometric Phase of the bottom of the layer relative to reference $z = 0$
- χ_a - Refractivity (index of refraction-1) for eigenstate a
- χ_b - Refractivity (index of refraction-1) for eigenstate b
- σ_a - Extinction coefficient for the a eigenpolarisation
- σ_b - Extinction coefficient for the b eigenpolarisation
- γ - Shape parameter of particles in the volume
- m_c - the backscatter coefficient from the volume

Hence we face a set of at least $9n$ physical parameters to totally characterise the multi-layer problem. A fixed frequency, single baseline polarimetric interferometer measures up to 36 parameters (the elements of P). Hence we see that, using this simplified argument, we might consider inversion up to 4-layer structures with such a single baseline system.

In practice, for small angle baselines in the absence of temporal decorrelation, we can assume that $T_{11} = T_{22}$ and hence only 27 parameters are available from P . Hence we are

limited to consider up to 3-layer structures. Nonetheless, many physical vegetation structures can be characterised in terms of a small number of distinct layers and hence are suitable candidates for this single base-line technology.

The most general formulation of polarimetric interferometry for an N-layer problem can then be written in compact matrix notation as

$$T_{11} = R_N (I_1^N + P_N R_{N(N-1)} (I_1^{N-1} + P_{(N-1)} R_{(N-1)(N-2)} (I_1^{N-2} + \dots) R_{(N-2)(N-1)} P_{N-1}^* \dots) R_{-N} \quad (21)$$

$$\Omega_{12} = R_N (e^{i\phi_N} I_2^N + P_N R_{N(N-1)} (e^{i\phi_{N-1}} I_2^{N-1} + P_{(N-1)} R_{(N-1)(N-2)} (e^{i\phi_{N-2}} I_2^{N-2} + \dots) R_{(N-2)(N-1)} P_{N-1}^* \dots) R_{-N} \quad (22)$$

$$I_1^i = e^{\frac{\sigma_{ai} + \sigma_{bi}}{\cos \theta_0} h_{vi}} \int_0^{h_{vi}} e^{\frac{\sigma_{ai} + \sigma_{bi}}{\cos \theta_0} z'} P(\tau_i) T_i P(\tau_i^*) dz' \quad I_2^i = e^{\frac{\sigma_{ai} + \sigma_{bi}}{\cos \theta_0} h_{vi}} \int_0^{h_{vi}} e^{ik_z z'} e^{\frac{\sigma_{ai} + \sigma_{bi}}{\cos \theta_0} z'} P(\tau_i) T_i P(\tau_i^*) dz' \quad (23)$$

$$\tau = v z = \left(\frac{\sigma_a - \sigma_b}{2} + ik(\chi_a - \chi_b) \right) \frac{z'}{\cos \theta_0} \quad (24)$$

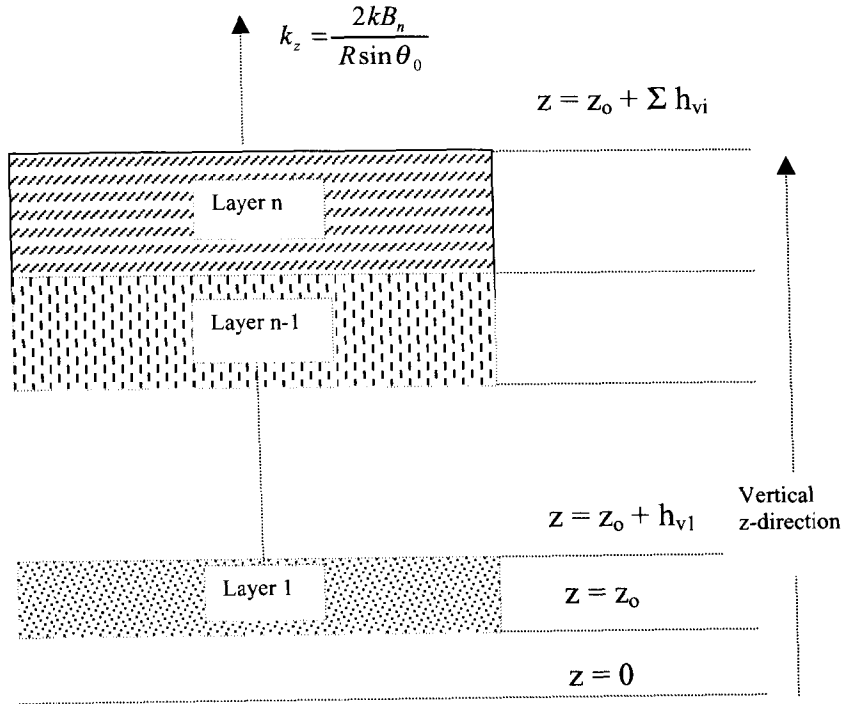


Figure 2 : General Layered Random Volume Scattering Geometry For Polarimetric Interferometry